Inorganic Chemistry

Article

pubs.acs.org/IC

High-Pressure and Theoretical Studies Reveal Significant Differences in the Electronic Structure and Bonding of Magnesium, Zinc, and Nickel Ions in Metalloporphyrinoids

Agnieszka Kania,[†] Mariusz Pilch,[†,‡] Dorota Rutkowska-Zbik,[§] Anna Susz,[†,‡] Heriyanto,[‡,∥] Grażyna Stochel,[†] and Leszek Fiedor*[,‡]

[†]Faculty of Chemistry, Jagiellonian University, ul. Ingardena 3, 30-060 Kraków, Poland

[‡]Faculty of Biochemistry, Biophysics and Biotechnology, Jagiellonian University, ul. Gronostajowa 7, 30-387 Kraków, Poland

[§]Jerzy Haber Institute of Catalysis and Surface Chemistry, Polish Academy of Sciences, ul. Niezapominajek 8, 30-239 Kraków, Poland

[∥]Ma Chung Research Center for Photosynthetic Pigments, Ma Chung University, Villa Puncak Tidar N-01, Malang 65151, Indonesia

Supporting Information

ABSTRACT: High pressure in combination with optical spectroscopy was used to gain insights into the interactions between Mg^{2+}, Zn^{2+}, and Ni^{2+} ions and macrocyclic ligands of porphyrinoid type. In parallel, the central metal ion−macrocycle bonding was investigated using theoretical approaches. The symmetry properties of the orbitals participating in this bonding were analyzed, and pigment geometries and pressure/ligation effects were computed within DFT. Bacteriopheophytin a was applied as both a model chelator and a highly specific spectroscopic probe. The analysis of solvent and pressure effects on the spectral properties of the model Mg^{2+}, Zn^{2+}, and Ni^{2+} complexes with bacteriopheophytin a shows that various chemical bonds are formed in the central pocket, depending on the valence configuration of the central metal ion. In addition, the character of this bonding depends on symmetry of the macrocyclic system. Since in most cases it is not coordinative bonding, these results challenge the conventional view of metal ion bonding in such complexes. In (labile) complexes with the main group metals, the metal ion−macrocycle interaction is mostly electrostatic. Significantly, water molecules are not preferred as a second axial ligand in such complexes, mainly due to the entropic constraints. The metal ions with a closed d shell may form (stable) complexes with the macrocycle via classical coordination bonds, engaging their p and s orbitals. Transition metals, due to the unfilled d shell, do form much more stable complexes, because of strong bonding via both coordination and covalent interactions. These conclusions are confirmed by DFT computations and theoretical considerations, which altogether provide the basis to propose a consistent and general mechanism of how the central metal ion and its interactions with the core nitrogens govern the physicochemical properties of metalloporphyrinoids.

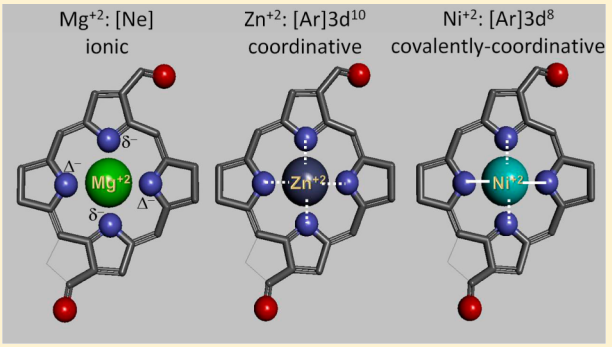

1. INTRODUCTION

The question of how atoms are bonded forming a molecule is a central issue in both experimental and theoretical chemistry, and naturally, the concept of chemical bonding has undergone a long evolution. The changing views of coordination bonds is an important example of such evolution, which influences many areas of chemistry and biology in which metal ion−ligand interactions are crucial for functioning. Metalloporphyrins are such typical coordination compounds, whose range of functions and applications is impressive, as it extends from them being catalytic centers in synthetic systems, through photosensitizing agents in photodynamic therapy and other applications, to key cofactors in many biological systems. Intensive efforts to comprehend both experimentally and theoretically the functioning of metalloporphyrins and their derivatives in various natural and man-made processes, along with the respective mechanisms involved, date back to the 19th century. Hemes and (bacterio)chlorophylls ((B)Chls), whose activity is dictated by the type of centrally coordinated metal ion, Fe^{2+} and Mg^{2+}, respectively, are the best representatives of this biologically important family of pigments. The Fe complexes either play the role of small-molecule carriers, such as O_2, CO_2, and NO, or participate in redox processes, while Mg-chelating (B)Chls are major photoactive cofactors of virtually all photosystems. In many systems that employ metalloporphyrinoids as cofactors, axial ligand binding is essential for their functioning. For instance, the binding of molecular oxygen to heme is axial ligand controlled, while axial coordination to the Mg center in (B)Chls serves to bind these cofactors to the

Received: May 7, 2014
Published: July 29, 2014

dx.doi.org/10.1021/ic501029b | Inorg. Chem. 2014, 53, 8473−8484

respective apoproteins. The mode of binding and the number of axial ligands are in large part predetermined by the type of bonding formed in the binding pocket of the porphyrinic chelators. Not only does the nature of this bonding determine the photophysical and chemical properties of the entire metallocomplex[1−3] but chelation substantially changes the coordinative properties of the metal center itself.[4,5] It is almost textbook knowledge that central metal ions (CMIs) in the metalloporphyrins and their derivatives are coordinatively bound in their central pockets. However, various metal ions form complexes of very different chemical stability, from very labile (Mg) to very stable (Ni, Fe, Co, etc.),[3] and the mechanisms underlying these effects of CMIs are largely unknown.

In the present paper, therefore, we have aimed at a precise description of the bonds formed in the porphyrinoid central pocket with different metal ions. In particular, we address the question of what is the electronic structure of the complexes formed by divalent metal ions and macrocyclic ligands of porphyrinoid type, applying metallosubstituted bacteriochlorophyll a (BChla) as a model metalloporphyrinoid, as studied by both theoretical and experimental approaches. In order to gain new insights into metal ion−tetrapyrrole bonding and the interactions of the CMIs with axial ligands, the effects of solvent and high pressure on axial ligand binding to BChla and its Zn- and Ni-analogues, Zn-BPheo and Ni-BPheo, and on its free base bacteriopheophytin a (BPheo, Figure 1) are investigated.

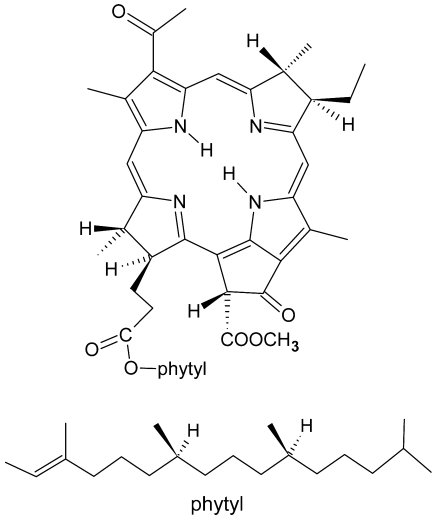

Figure 1. Structural formula of bacteriopheophytin a, the free base of bacteriochlorophyll a (BChla).

Here, moderately high hydrostatic pressure (up to 2000 bar) is applied to enhance pigment−solvent interactions, in particular interactions with axial ligands, without affecting the electronic structures of the species involved. The unique spectral properties of BChla, i.e., the high sensitivity of its well-separated electronic transitions (Q_Y and Q_X) to solvation and axial ligation (see Figure 2), make it possible to use the pigment as both a biologically relevant chelator and a spectroscopic probe. In particular, the S_2 electronic level (Q_X) in BChla is strongly coupled to the ligation state of the CMI; it peaks near 570−580 nm in the pentacoordinated form and shifts to 610−620 nm upon binding of the second axial ligand.[6−8] Importantly, this feature of the chelator allows for an easy spectroscopic detection of subtle single chemical events, such as

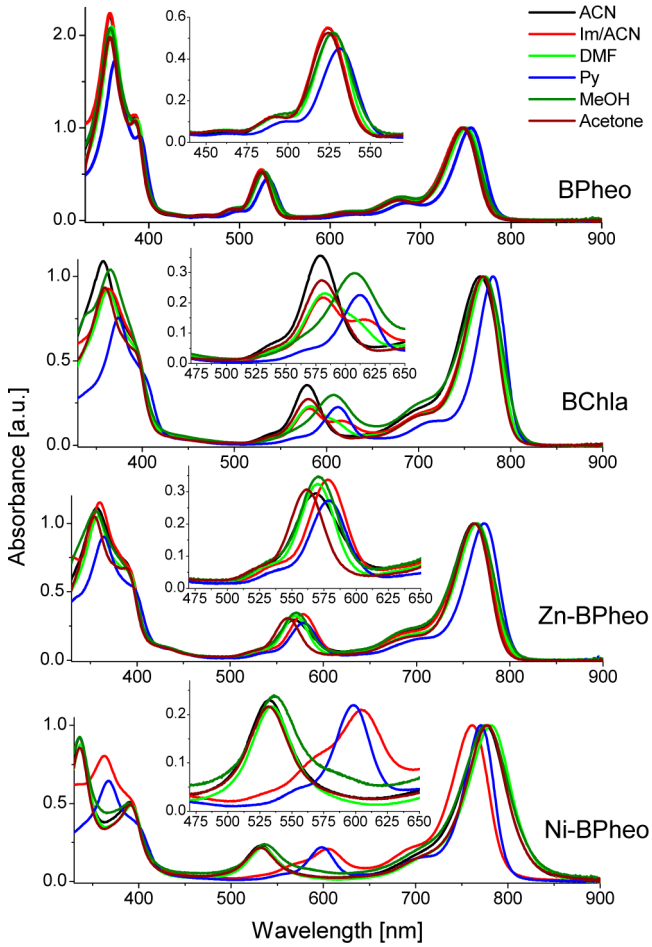

Figure 2. Electronic absorption spectra of bacteriopheophytin a (BPheo), bacteriochlorophyll a (BChla), and its Zn- and Ni-substituted analogues, Zn-BPheo and Ni-BPheo, recorded in solvents of varying coordination strength: acetonitrile (ACN), 154 mM imidazole in acetonitrile (Im/ACN), dimethylformamide (DMF), pyridine (Py), methanol (MeOH), and acetone. The spectra were normalized to the Q_Y maximum. The expanded regions of the Q_X transition in the insets show spectral changes related to the coordination state of the central metal ions.

solvation, or events taking place at the CMI: a loss or binding of axial ligands. It has been fruitfully exploited in earlier model studies.[5,9−15] The free base BPheo was used as as a reference chromophore, in which solvation effects can be observed without interference from axial ligand effects. In parallel, CMI−tetrapyrrole bonding was investigated by theoretical approaches. The symmetry properties of the orbitals participating in this bonding were analyzed, and the pigment geometries and the effects of axial ligands were computed within time-dependent density functional theory (DFT).

Our analysis of the solvent and high-pressure effects on the model complexes shows that various metal ions form very different types of bonds with the central pocket nitrogens, depending on their valence electronic configuration and the symmetry properties of the macrocyclic chelator. Because in most cases it is not bonding of the coordinative type, these results challenge somewhat the common view. In addition, a consistent mechanism is proposed of how the type of central metal ion determines the coordinative and physicochemical properties of the entire metallocomplex.

dx.doi.org/10.1021/ic501029b | Inorg. Chem. 2014, 53, 8473−8484

2. RESULTS

2.1. Solvent and Pressure Effects on the Absorption Spectra. *Solvent Effects.* The electronic absorption spectra of BPheo, BChla, Zn-BPheo, and Ni-BPheo were recorded in several organic solvents of varying ligation strength, from weakly coordinating acetonitrile (ACN), to moderately coordinating dimethylformamide (DMF), to strongly ligating methanol (MeOH), imidazole (Im) in ACN, and pyridine (Py). The spectra are presented in Figure 2, in which the insets show the expanded Q_X region. The positions of the absorption maxima are in agreement with values reported earlier.[8,11,16] Among the model pigments, the absorption spectrum of the free base shows the weakest solvent effect. Its absorption maxima are the most red-shifted in Py, and the higher the energy of the transition, the larger the shift (with respect to their positions in ACN). The absorption maxima of the Zn complex show a slightly stronger solvent effect, while those of BChla and Ni-BPheo are the most affected. Their Q_Y transitions shift by more than 300 cm^{-1}, and in the latter case the Soret components are characteristically split in weakly coordinating solvents. In both pigments, the Q_X band is considerably solvent-sensitive and shows a multicomponent character. For instance, in the spectrum of Ni-BPheo in ACN, upon the addition of Im (154 mM), two new bands appear, a weaker one at 570 and a stronger one at 604 nm. In the spectrum of BChla in the same solvent a new shoulder appears at 614 nm. This lower energy Q_X component of the BChla spectrum becomes dominant in MeOH and Py, and similarly for Ni-BPheo in Im/ACN and Py. Obviously, these spectral changes reflect the changes in the axial coordination.[6−8] Importantly, Ni-BPheo is the only pigment having three coordination forms, in which the central Ni^{2+} ion is four-, five-, and six-coordinated, respectively.

Water Molecules As the Axial Ligands. The shapes of Q_X of BChla in several aqueous solvent systems at atmospheric pressure are shown in Figure 3. The addition of water (up to 10%, 5.6 M) to ACN does not affect its maximum at 578 nm but causes a slight increase in absorption near 620 nm, which indicates the occurrence of a small population of hexacoordinated pigment. However, the effect of water is several orders of magnitude weaker than that caused by Im (154 mM) in the same solvent. Similarly, in a highly aqueous detergent solution (0.3% Triton X-100), the Q_X band of monomeric BChla, peaking at 586 nm, shows practically no asymmetry, and even an increase of pressure to 2000 bar has no effect on the band shape, in contrast to other ligands in organic media (see below and in Figure S1, Supporting Information). This shows that the water molecule is a weak ligand, unable to bind to the central Mg^{2+} ion at the second axial position.

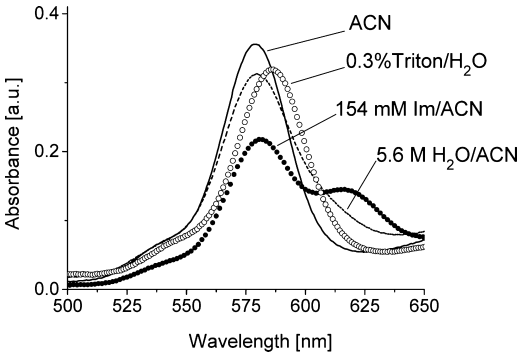

Figure 3. Shape of the Q_X band of bacteriochlorophyll a recorded in acetonitrile and in acetonitrile containing either imidazole (154 mM) or water (5.6 M), compared to a micellar environment of 0.3% Triton X-100 in water.

Pressure Effects on Electronic Transitions. The pressure-induced shifts of the main absorption transitions of BPheo, BChla, Zn-BPheo, and Ni-BPheo are plotted in Figure 4, and

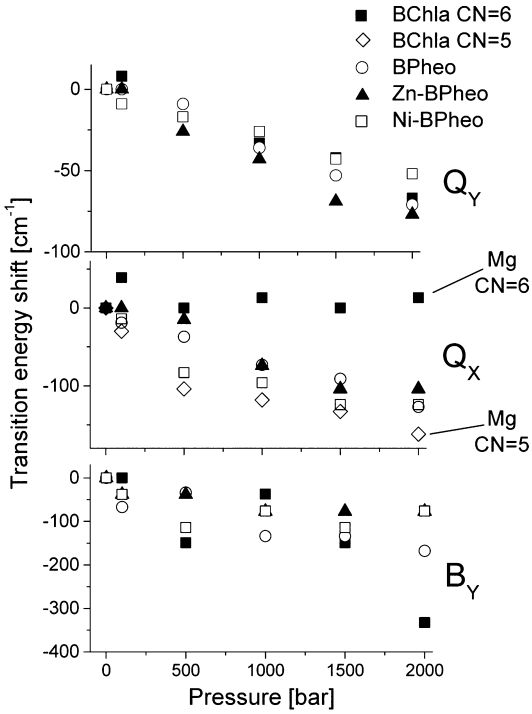

Figure 4. Pressure effects on the energies of the main absorption transitions (Q_Y, Q_X, and B_Y), of bacteriopheophytin a (BPheo), bacteriochlorophyll a (BChla), and its Zn- and Ni-substituted analogues, Zn-BPheo and Ni-BPheo, recorded in acetonitrile containing 154 mM imidazole. The plots were normalized to zero value at 1 bar. Note the differences in the behavior of the Q_X transitions corresponding to the penta- and hexacoordinated Mg complex (CN = coordination number). The exact values of the Q_X maxima were obtained via spectral deconvolution (see the text for details).

the values of the slopes of all transition energy−pressure plots are collected in Table S1 (Supporting Information). In organic solvents, an increase in pressure from ambient to 2000 bar results in a few nanometer red shift of the Soret and Q_Y bands. Similar shifts, along with a small (3 nm) red shift of the Q_X band, are observed in the spectra of BPheo and BChla in the micellar system (Figure S1). The band energies decrease linearly with pressure, and, in general, the higher the transition energy, the larger the pressure effect (Figure 4, Table S1). Except these shifts, in this range of pressures, the absorption transitions undergo no other changes; for example, the bandwidths remain the same (not shown).

Spectral deconvolution, done as previously described,[5] shows that the electronic transitions of all four pigments in the Im/ACN system are sensitive to pressure in a similar way, with the notable exception of hexacoordinated BChla, whose Q_X energy seems to be unaffected by pressure (Figure 4).

Axial Ligation under Pressure. In several cases, pressure characteristically affects the shape of the Q_X band (Figure S1).

dx.doi.org/10.1021/ic501029b | Inorg. Chem. 2014, 53, 8473−8484

Table 1. Effects of High Pressure on the Ratio between the Coordination Forms of BChla, Zn-BPheo, and Ni-BPheo in Weakly and Strongly Coordinating Solvent Systems, Estimated by Spectral Deconvolution[a]

	BChla				Zn-BPheo		Ni-BPheo					
	pressure [bar]											
	1		2000		1	2000	1			2000		
	% of pigment coordination form											
	5	6	5	6	5	5	4	5	6	4	5	6
ACN	97	3	82	18	100	100	87	13	0	87	13	0
ACN+Im	69	31	57	43	100	100	16	41	43	16	28	56
DMF	69	31	61	39	100	100	82	18	0	82	18	0
MeOH	26	74	33	67	100	100	90	10	0	84	16	0
Py	23	77	25	75	100	100	11	33	56	13	34	53

[a]See the text for details.

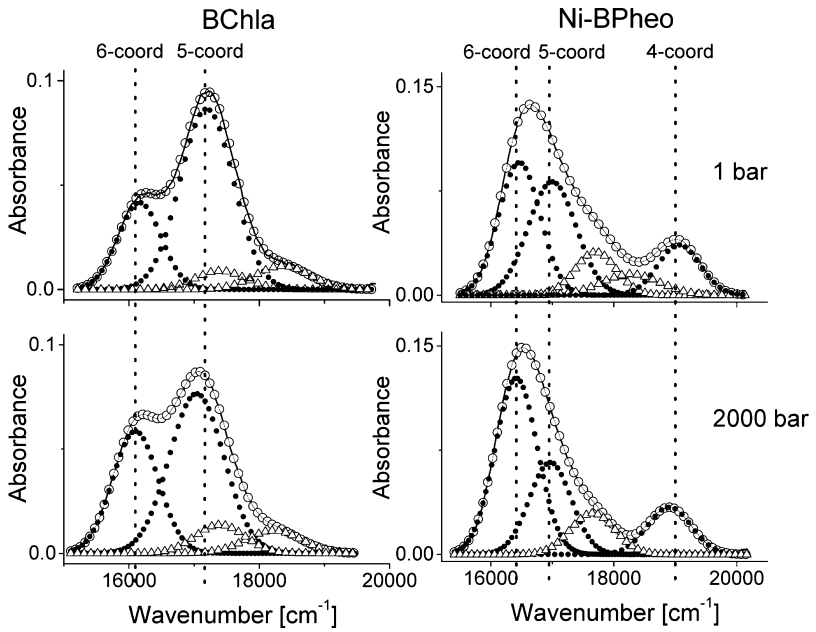

Figure 5. Deconvolution of the Q_X spectral region of bacteriochlorophyll a (BChla) and its Ni-substituted analogue (Ni-BPheo), measured in acetonitrile containing 154 mM imidazole under atmospheric and high hydrostatic pressure (2000 bar). The deconvolution was done with Gaussian−Lorentzian curves (see the text for details). Legend: (○) experimental data; (−) sum of the fitted components; (●) resolved Q_X transitions (0−0); and (△) resolved Q_X vibrational sidebands.

For BChla in ACN, Im/ACN, or DMF it becomes asymmetrical and an additional component appears on its low-energy side. In the case of Ni-BPheo, changes within Q_X are visible only in Im/ACN; its major component grows at the expense of the band centered at 570 nm, while the one at 535 nm remains unaffected. In order to estimate the contribution of individual coordination forms, deconvolution of the Q_X band into Gaussian−Lorentzian components was applied.[5] The results of this analysis are summarized in Table 1, and, as an example, deconvolution of the Q_X bands in the spectra of BChla and Ni-BPheo in Im/ACN under pressure is shown in Figure 5. The pressure does not affect the shape of the Q_X band of the free base, having a single Gaussian−Lorentzian component (plus the vibrational sidebands, not shown). Similarly, irrespective of solvent and pressure, only one Q_X component was found for Zn-BPheo, corresponding to a single axial coordination form (penta). In the case of Mg^{2+} and Ni^{2+} complexes, more components were found under the Q_X envelope, and high pressure affects the ratio between these components, indicating shifts in the coordination equilibria (Figure 5, Table 1).

In ACN, as expected, an increase in hexacoordinated BChla is observed, from 3% (1 bar) to 18% (2000 bar), and a smaller one in Im/ACN or DMF. In MeOH and Py, however, an opposite trend is observed, i.e., an increase in pentacoordination at the expense of hexacoordination. In Ni-BPheo, increased pressure does not affect the coordination equilibria in ACN, DMF, and Py, but there is a slight shift toward pentacoordination in MeOH and toward hexacoordination in Im/ACN. In all cases, the relative amount of the nonligated form of Ni-BPheo does not depend on pressure.

Reaction Volumes. The ligation equilibria of BChla and Ni-BPheo in solution can be described as follows:

$$\text{BChla-L}_1 + \text{L}_2 \leftrightarrow \text{BChla-L}_1\text{-L}_2 \quad (1)$$

$$\text{Ni-BPheo} + \text{L}_1 \leftrightarrow \text{Ni-BPheo-L}_1 \quad (2)$$

$$\text{Ni-BPheo} - \text{L}_1 + \text{L}_2 \leftrightarrow \text{Ni} - \text{BPheo-L}_1\text{-L}_2 \quad (3)$$

dx.doi.org/10.1021/ic501029b | Inorg. Chem. 2014, 53, 8473−8484

Table 2 lists the values of ΔV, i.e., the change in reaction volume associated with the overall ligation reaction characterized by the equilibrium constant K, calculated on the basis of the following relationship:

Table 2. Reaction Volume Changes ΔV Associated with Axial Ligation of BChla and Ni-BPheo in Weakly and Strongly Coordinating Solvent Systems, Calculated Considering Spectral Changes Due to Pressure Increasing Stepwise from 1 to 2000 bar[a]

		ΔV [cm^3/mol]	
solvent	ligation	BChla	Ni-BPheo
ACN	4 ↔ 5		−1.0 ± 0.2
	5 ↔ 6	−24.5 ± 1.4	
ACN+Im	4 ↔ 5		−1.3 ± 0.9
	5 ↔ 6	−7.0 ± 0.5	+0.1 ± 0.6
DMF	4 ↔ 5		+1.7 ± 0.1
	5 ↔ 6	−4.0 ± 0.7	−0.6 ± 0.4
MeOH	4 ↔ 5		−3.4 ± 0.8
	5 ↔ 6	+4.3	
Py	4 ↔ 5		+0.5 ± 0.9
	5 ↔ 6	+0.9 ± 0.7	+1.3 ± 0.8

[a]Only for BChla in MeOH were the ΔV values estimated on the basis of the two terminal points, i.e., 1 and 2000 bar (see the text for details).

$$(\delta \ln K/\delta p)_T = -\Delta V/RT \ [\mathrm{cm^3/mol\cdot K}]$$

as derived from $(\delta G/\delta P)_T = V$. The K values were estimated from the contributions of the respective coordination forms in the equilibrium mixtures, as determined via spectral deconvolution (see Figure 5). The ΔV of the sixth ligand binding to BChla changes from negative (in ACN and DMF) to positive (in MeOH and Py) and ranges from −24.5 cm^3/mol in ACN to +4.3 cm^3/mol in MeOH (Table 2). The ΔV values estimated for ligation to Ni-BPheo vary within a narrower range, from −3.4 cm^3/mol in MeOH to +1.7 cm^3/mol in DMF, also changing sign but in most cases being close to zero.

Correlation between Transition Energies. Table 3 presents the effects of hydrostatic pressure on the correlation between the energies of the Q_Y and Q_X transitions (transition energy correlation factor, ECF), the two best resolved in the absorption spectra, as determined in several solvents. The exact positions of Q_X maxima in the metallocomplexes, corresponding to particular coordination forms, were determined via band deconvolution, as described above. In all cases, the ECFs change linearly with pressure. In BPheo the EFC equals 0.6 and is practically solvent-independent, whereas in the metallocomplexes the ECFs depend on both the axial coordination number and the solvent. In hexacoordinated BChla, when the pentacoordinated form is also present, ECF increases to 1. However, in MeOH and Py, in which hexacoordination predominates, ECF equals ∼0.6, as in the pentacoordinated BChla, except in DMF. In this solvent, for both coordination forms, ECF is even lower. In Zn-BPheo it depends to some extent on the solvent and ranges from 0.51 to 0.85. Owing to the separation of the respective Q_X transitions in the spectrum of Ni-BPheo, all three coordination forms of the pigments could be resolved. Thus, in all solvents except Py, ECF in the pentacoordinated form is lower than that in the other two forms. In Py, the trend is different; that is, ECF increases from 0.26 through 0.44 to 0.52 for the four-, five-, and six-coordinate form, respectively.

2.2. Geometry Structures of BPheo and Its Metallocomplexes. The applied time-dependent DFT formalism provides an acceptable level of prediction of electronic transition energies in cyclic tetrapyrrolic systems with reasonable computational time.[17,18] The typical error in bond length determination using the current DFT method is 0.01 Å, and its results agree very well with the experimentally determined values (see the Discussion). Thus, the method combines a high accuracy with relatively low costs of computations, which is highly relevant considering the complexity of such macrocyclic systems. The results of the DFT-based prediction of the geometry structures of ligated BChla, Zn-BPheo, and Ni-BPheo in a series of solvents are summarized in Table 4. The axial ligands in the Mg^{2+} and Zn^{2+} complexes (pentacoordination) form relatively long bonds, which span 2.11 to 2.43 Å, while the central Ni^{2+}−axial ligand distances are generally shorter, between 1.98 and 2.24 Å.

The lengths of the axial bonds vary for different ligands, but they do not seem to be correlated with ligand strength. As a rule, if the same ligands are compared, the CMI−ligand bonds are shorter in pentacoordinated complexes than in the hexacoordinated ones, as for instance in complexes with methanol: 2.15 Å vs 2.24 Å (Table 4). In all pentacoordinated complexes, a significant, i.e., ∼0.30−0.35 Å, out-of-plane

Table 3. High-Pressure Effects on the Correlations between the Q_Y and Q_X Energies (Transition Energy Correlation Factors, ECFs) in BPheo, BChla, Zn-BPheo, and Ni-BPheo in Organic Solvents[a]

solvent	BPheo	Mg-BChla	Zn-BPheo	Ni-BPheo
ACN	0.58 ± 0.04	**6**: 1.19 ± 0.16	0.74 ± 0.02	**5**: 0.62 ± 0.25
		5: 0.51 ± 0.04		**4**: 0.82 ± 0.05
ACN+Im	0.61 ± 0.04	**6**: 0.88 ± 0.10	0.63 ± 0.06	**6**: 0.49 ± 0.05
		5: 0.53 ± 0.04		**5**: 0.31 ± 0.13
				4: 0.47 ± 0.14
DMF	0.59 ± 0.09	**6**: 0.38 ± 0.03	0.85 ± 0.07	**5**: 0.49 ± 0.15
		5: 0.24 ± 0.03		**4**: 0.72 ± 0.11
MeOH	0.58 ± 0.07	0.58 ± 0.08	0.62 ± 0.14	**5**: 0.15 ± 0.02
				4: 0.42 ± 0.05
Py	0.61 ± 0.03	0.61 ± 0.05	0.51 ± 0.04	**6**: 0.52 ± 0.08
				5: 0.44 ± 0.08
				4: 0.26 ± 0.08

[a]The values of SD errors are also indicated. The bold numbers indicate the coordination numbers of the central metal ions.

dx.doi.org/10.1021/ic501029b | Inorg. Chem. 2014, 53, 8473−8484

Table 4. DFT (BP/def-TZVP) Geometry Parameters of the Plausible BChla, Zn-BPheo, and Ni-BPheo Adducts with Several Ligands of Various Coordination Strength

system	metal−ligand bond [Å]	displacement [Å]
BChla(ACN)	2.24	0.32
BChla(ACN)$_2$	2.38, 2.37	
BChla(Im)	2.20	0.38
BChla(Im)$_2$	2.33, 2.34	
BChla(DMF)	2.11	0.36
BChla(DMF)$_2$	2.24, 2.26	
BChla(MeOH)	2.15	0.30
BChla(MeOH)$_2$	2.24, 2.24	
BChla(Py)	2.24	0.36
BChla(Py)$_2$	2.39, 2.43	
Zn-BPheo(ACN)	2.26	0.30
Zn-BPheo(Im)	2.16	0.36
Zn-BPheo(DMF)	2.19	0.30
Zn-BPheo(MeOH)	2.25	0.23
Zn-BPheo(Py)	2.20	0.35
Ni-BPheo(ACN)	1.98	0.29
Ni-BPheo(Im)	2.05	0.27
Ni-BPheo(Im)$_2$	2.18, 2.18	
Ni-BPheo(DMF)	2.08	0.23
Ni-BPheo(MeOH)	2.12	0.20
Ni-BPheo(Py)	2.06	0.29
Ni-BPheo(Py)$_2$	2.21, 2.24	

displacement of the CMI is found, but, again, the displacement does not seem to be related to the length of the CMI−ligand bond. Importantly, the computations for the hexacoordinated Zn-BPheo consistently yielded axial bonds that are 0.3−0.4 Å longer (not shown) than the respective bonds in the pentacoordinated complexes, indicating high instability of the hexacoordinated species, in agreement with the experimental result. Analogously, the strength of these bonds differs in the five- and six-coordinate complexes of BChla,[5] which can be attributed to the trans influence of axial ligands.

Simulation of Pressure Effects on Spectral Shifts. In order to account for pressure-induced bathochromic shifts in the absorption spectra, the TD-DFT method was applied to simulate the spectra of BChla in ACN. Because an increase in pressure is expected to cause a shortening of the CMI−ligand bond and, in the case of pentacoordination, a return of the metal ion to the molecular plane, in the present *in silico* experiment, the energy of the first singlet excited state of BChla was computed for the following systems: (i) the geometry-optimized BChla−ACN complex; (ii) the BChla−ACN complex in which the Mg^{2+}−ligand bond is shortened by 10% of its optimal length; and (iii) the BChla−ACN complex where Mg^{2+} is forced into the plane of the macrocycle and the length of the axial bond is either reduced by 10% or left unchanged. The results of the computations are shown in Table 5 as the shifts of the Q_Y transition. The band position is independent of the CMI position, but it shifts due to bond shortening, indicating that the effects of pressure on transition energies are related to the Mg^{2+}−ligand distance, rather than to a deeper insertion of Mg^{2+} into the tetrapyrrole plane.

2.3. Symmetry Properties. In cyclic tetrapyrrolic chelators, CMI binding in the central pocket results from its interaction with eight electrons delivered by the core nitrogens. The system of conjugated double bonds in porphyrin and Pheo/BPheo anions has a strict D_{4h} and C_1/C_{2h} symmetry,

Table 5. Theoretical Simulation of High-Pressure Effect on the Lowest Energy Electronic Transition of BChla in ACN[a]

bond length [Å]	Mg^{2+} position	band shift
90% R_0	out of plane	+3 nm (−64 cm^{-1})
R_0	in plane	0
90% R_0	in plane	+2 nm (−43 cm^{-1})

[a] R_0 corresponds to the Mg−ligand distance in the equilibrium structure, equal to 2.24 Å.

respectively. In all these molecules the central binding pocket is formed by four nitrogen atoms whose valence electrons also strongly contribute to the extensive system of delocalized π-electrons, making a description of the ligand field and its symmetry in such complexes less straightforward. Many additional factors, such as reduced rings, which partly freeze the pattern of the conjugated C=C bonds, and peripheral functional groups, determine its symmetry. In addition, the distribution of charges around the CMI is very sensitive to environmental factors. The shift of the CMI above the molecular plane also lowers the symmetry. In effect, the charges on the two opposite core nitrogens differ, indicating a $C_{2h}/C_{2v}/C_2$ symmetry of the ligand field, as seen in previous theoretical and experimental works and more recently in our calculations.[14]

3. DISCUSSION

3.1. Choice of Model System. Chls and BChls are in most instances referred to and investigated in their photosynthetic context. In this work, however, we attempted to exploit BChla in a less traditional way, as a remarkably specific spectroscopic probe, highly sensitive to both coordination state of the CMI and solvation, being at the same time the macrocyclic ligand. Another advantage of using BChla is its capacity to host various divalent metal ions; the Mg^{2+}, Zn^{2+}, and Ni^{2+} ions were chosen as the CMIs because of their precisely defined coordination states and the lack of redox states under ambient conditions. In addition, moderately high hydrostatic pressure, another basic parameter that thermodynamically defines the state of a system, has been used to intensify intermolecular interactions of metallocomplexes to reveal the details of their electronic structure.

3.2. Computational Approach. Theoretical and computational studies on (B)Chls in relation to their key role in photosynthesis have a long track record.[17−25] At least equally long is the history of theoretical investigations of metalloporphyrins, as reviewed extensively.[26−29] However, not many studies addressed the character of chemical bonding in the core of these macromolecular chelates.[30−33] Such an analysis is undertaken in the present computational approach. Its validity can be evaluated based on the comparison with the values obtained in high-resolution X-ray crystallographic studies on pigment−protein complexes containing BChla, in particular photosynthetic reaction centers and antenna complexes. For instance, the His−Mg^{2+} distances fall between 1.9 and 3.2 Å for the special pair of BChls[34] and 2.3 Å for B850 in LH2 antenna.[35,36] Similar values are found in the crystal structures of plant or cyanobacterial photosynthetic complexes, e.g., in LHCII,[37] photosystem I,[38] and photosystem II.[39] Somewhat longer bond lengths, between 3.4 and 3.7 Å, were found for Ser as the ligand. In both cases, the values computed for the Im−BChla and MeOH−BChla complexes (Table 4) are very close to those found experimentally. There are no structural data on

dx.doi.org/10.1021/ic501029b | Inorg. Chem. 2014, 53, 8473−8484

Zn- and Ni-substituted BChla, but the computed coordination bond lengths in these complexes compare very well to the data obtained for Zn-porphyrins and Zn-bacteriochlorin and for Ni-porphyrins.[34,40−42] Moreover, the present calculations correctly predict the instability of hexacoordinated Zn^{2+} complexes (see below).

3.3. Solvation Effects. The free base BPheo can be considered a reference chromophore, helpful in assessing both solvation and the effects of pressure, in the absence of axial coordination. A comparison of the absorption spectra in Figure 2 and very similar sensitivities of the electronic transitions to pressure (Figure 4) show that the Zn complex undergoes a similar solvation to that of BPheo. In the Mg and Zn derivatives both solvent and pressure cause changes in the coordination state of the CMI, as shifts in and splitting of the Q_X band reveal (Figures 2, 3, and 4). The plots of transition energy−pressure relationships (slopes listed in Table S1) provide a more quantitative means for comparison of pressure effects on solvation. The narrow range of slope values, between 0.030 and 0.045 cm^{-1}/bar (somewhat lower in the micellar system, 0.02 cm^{-1}/bar), determined for the Q_Y band indicates that pressure similarly weakly affects S_1 energies in all pigments, irrespective of the solvent system and the CMI. Practically the same weak effect of pressure on S_1 energy in BChla has been noted previously.[43] The main components of the Soret band, i.e., B_X and B_Y, show somewhat higher sensitivity to pressure (steeper slopes, Table S1), but in all cases the pressure dependence is similar to that in BPheo, indicating that shifts in the S_1 and S_3 state energy are related to solvation rather than to axial coordination, in contrast to the S_2 state. This increased sensitivity of higher excited states of (B)Chls to environmental factors has been seen previously.[11,43]

The generally weak effect of pressure (and solvation) on the position of the electronic transitions of the pigments can be explained by the nature of solvent−chromophore interactions. According to a previous study,[44] pressure-induced shifts result from a combination of attractive and repulsive interactions between solvent and pigment molecules. The present DFT-based quantification of the interaction/solvation energy for BPheo gives a value of ca. 2 kcal/mol, irrespective of the solvent. This value indicates very weak bonding between the chromophore and solvent molecules, e.g., of the van der Waals type.

3.4. Axial Coordination. The spectral deconvolution in the Q_X region allows an estimation of the respective equilibrium constants and subsequently the estimation of activation volumes for ligation of the pigments under pressure. The measured ΔV values are quite low, with the single exception of ACN, being well below −10 cm^3/mol, a value typically associated with the formation of covalent bonds.[45] This range of ΔV values is consistent with the formation of coordination bonds, obviously weaker than covalent ones.

The substantially larger ΔV found for BChla ligation in ACN can be adequately explained by the compressibility of the ACN−BChla complex, which results from the fact that ACN is only a weak electron donor, expected to carry no significant steric effects (other ligands used are much bulkier). Thus, as the present calculations predict, the ACN−Mg^{2+} distance can be shortened to a higher degree than that of other ligands (Table 4). Seemingly, the electrostatic repulsion at the core does not increase when an electron is donated by such a weak donor, even under high external pressure. This changes when the ligands are strong electron donors, such as Im and Py. Apparently, in this case, the repulsion at the core must be considerably stronger, in line with the intriguing fact that under higher pressure the ligation equilibrium is pushed toward pentacoordination, and the stronger the ligand, the less hexacoordination is favored under pressure. This observation runs somewhat counter to common sense, as pressure is expected to favor hexacoordination.

In general, the binding energy of the first axial ligand is much higher than the ligand−CMI interaction in the hexacoordinated complex, as shown experimentally[5,11,46] and now in DFT-based computations (Table 4). In addition, as discussed below, the binding of a second axial strong ligand requires some rebuilding of the valence configuration on the metal center. However, under external pressure, due to a stronger interaction between the first ligand and the CMI, the pentacoordinated complex gains additional stability. In effect, the rebuilding of the CMI valence orbitals becomes more difficult, and at the same time a stronger repulsion between the core and the electrons from the approaching second ligand occurs. This is in line with the occurrence of repulsive interactions at the core of Ni-BPheo, shown both experimentally and computationally.[10] Hence, under pressure the ligation equilibrium shifts toward pentacoordination.

The changes in ΔV sign agree well with the rebuilding of the valence orbitals of the CMI upon hexacoordination. The negative sign of ΔV, as found in most cases, relates to a decrease in the partial volume of reactants due to the formation of coordination bonds. The change of the ΔV sign to positive, observed for strong ligand binding to Mg and Ni complexes, speaks for valence configuration rebuilding (or hybridization[15]), leading to an increase of the partial volume of hexacoordinated complexes. Such an expansion is clearly seen also in the present calculations as a lengthening of the CMI−axial ligand bond (Table 4).

3.5. Correlation between Transition Energies. The ECF between the energies of perpendicularly oriented electronic transitions is a useful descriptor of molecular distortion of tetrapyrrolic chromophores.[11,47] The present approach, in which pressure effects are analyzed, differs from the one usually taken, where solvent effects are considered, but the ECF values may provide an estimation of pressure-related molecular distortions. In principle, if similar chromophores are considered, the lower the factor, the larger the deformation. In BPheo the ECF value (∼0.6) is solvent-independent, seemingly because solvation under pressure does not affect the geometry of the molecule, whose planarity can be assumed on the basis of crystallographic studies on model compounds and can be treated as a reference. On the basis of somewhat higher ECF values, a degree of distortion is expected to occur in Zn-BPheo in the presence of weak ligands. A decrease in its value in Im, in MeOH, and particularly in Py shows that the binding of strong ligands causes greater deformation, probably due to CMI displacement. Such a displacement is seen in the crystal structure of Zn-bacteriochlorin[41] and confirmed in the present computations (Table 4). In a monoligated Mg complex a considerable macrocycle deformation due to pressure can be seen, and the stronger the ligand, the more significant it is. When both axial positions are occupied, a return to planarity is seen and consequently ECF increases. The relatively low values of ECF for deligated Ni-BPheo indicate that with no axial ligand the complex assumes a nonplanar conformation. Except in Py, ECF values decrease due to the binding of the first axial ligand, showing an even larger deviation of the chromophore.

dx.doi.org/10.1021/ic501029b | Inorg. Chem. 2014, 53, 8473−8484

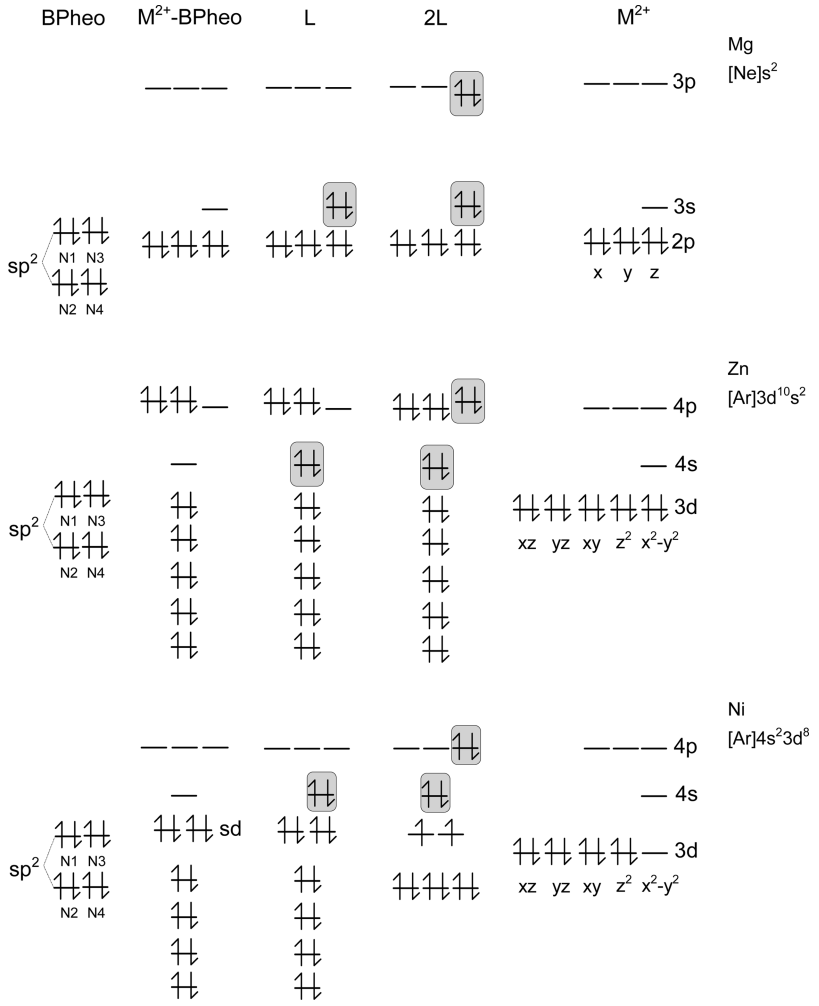

Figure 6. Schematic presentation of electron distribution on the valence orbitals of the core nitrogen atoms (N1−N4) and the central metal ions, which contribute to bond formation in the central cavity, in bacteriopheophytin a (BPheo) and its Mg, Zn, and Ni complexes (M^{2+}-BPheo). Also, the electrons of the axial ligand(s) (L) and the valence orbitals of the metal ions are shown. The gray boxes indicate the electron pairs involved in the bond formation.

The binding of Im as the second axial ligand brings the molecule to planarity, while in the case of Py, a significant change in electron distribution on the metal center occurs and a return to planarity is seen in both the mono- and biligated complexes.

3.6. Central Metal Ion−Macrocycle Bonding. Analysis of the symmetry properties of orbitals possibly involved in chelator−metal ion bonding shows that effective bond formation will depend both on ligand field symmetry and on the symmetry properties of the valence orbitals of CMI. In the case of the D_{4h} and C_{2h} symmetry of the chelator (in the anionic form), the wavefunction of its π-electron system including core nitrogens is odd (u), while the CMI d orbitals possess an even (g) symmetry due to the inversion operator, and formally these two systems cannot interact with each other because the orbitals p and d do not belong to the same representation. This implies that in metallocomplexes of porphyrin^{2-} (D_{4h}) and BPheo^{2-} (C_{2h}) the valence orbitals of CMI only weakly interact with the molecular orbitals of the π-electron systems. Any effective interaction (= bonding) between these two systems becomes possible only when the chelator symmetry is lowered. As discussed below, the nature of this bonding strongly depends on the symmetry properties of the valence orbitals of CMI (Figure 6).

Bonding to Mg^{2+}. The spherical Mg^{2+} ion has a very stable electronic configuration, equivalent to that of neon; that is, the inner shells (n = 1 and 2) are fully occupied, and the closed-shell electrons will not tend to form bonds (Figure 6). The core nitrogens would thus be able to donate their electrons to the empty shell 3, except that its energy happens to be too high, which is unfavorable to the formation of the N−Mg^{2+} coordination bond. Hence, the bonding interaction with tetrapyrrolic chelators is expected to be mostly of an electrostatic (ionic) character. This is consistent with the high lability of the central Mg^{2+} in (B)Chls, which is easily removed already at pH near 6. A recent theoretical study also shows that the exchange of Mg^{2+} for protons is energetically advantageous.[48] In Mg^{2+} complexes, some degree of electrostatic repulsion between the core electrons and the sp^2 electrons on central nitrogens must be expected, which explains the well-known out-of-plane displacement of the central Mg^{2+} in (B)Chls. The repulsion effect is enhanced when the central Mg^{2+} accepts axial ligands (see below).

Bonding to Zn^{2+}. The electronic structure of spherical Zn^{2+} is similar to that of Mg^{2+} in the respect that is has a fully

dx.doi.org/10.1021/ic501029b | Inorg. Chem. 2014, 53, 8473−8484

occupied shell (n = 3). However, Zn^{2+} complexes with tetrapyrrolic macrocycles are much more stable than Mg^{2+} complexes. This indicates a much stronger interaction between core nitrogens and the metal ion via the donation of sp^2 electrons, seemingly, to the empty orbitals of shell 4 of the latter (Figure 6). The formation of this coordination bond is possible because the energy of shell 4 orbitals, lower than the energy of shell 3 in Mg^{2+}, is close to the energy of the sp^2 orbitals. For geometrical reasons, three orbitals of shell 4, namely, 4s, $4p_x$, and $4p_y$, may contribute to the formation of $N-Zn^{2+}$ bonds and four pairs of sp^2 electrons compete for these three orbitals. Both energetic and geometric factors will cause the coordination of Zn^{2+} to be most favorable in planar complexes, which is confirmed in the present calculations. The smaller core size of the Zn^{2+} ion also results in smaller repulsion with the sp^2 electrons (see below).

Bonding to Ni^{2+}. As shown in our recent work, a nonspherical symmetry and the presence of empty 3d and 4s orbitals in the central Ni^{2+} ion create new possibilities for bond formation with the tetrapyrrolic chelator.[15] The $d_{x^2-y^2}$ and s orbitals seem to form two sd hybrids, which may accept two electrons each from the sp^2 orbitals, forming two three-center bonds of a strong covalent character. An effective overlap will take place in particular for electrons coming from diagonally situated core nitrogens. Additional weak bonding of a coordinative character occurs because the remaining two sp^2 orbitals may donate electrons to the coplanar $4p_x$ and $4p_y$ orbitals (Figure 6). As a result, Ni^{2+} complexes are of exceptional chemical stability among metallosubstituted (B)Chls.[15] Large energetic costs of Ni^{2+} removal were also predicted theoretically.[49]

3.7. Axial Ligand Binding. *Mg Complexes.* The binding of axial ligands to the central Mg^{2+} in (B)Chls is feasible via its empty 3s and $3p_z$ orbitals, which both have suitable directional properties. If a complex with a single axial ligand is formed, the ligand lone electron pair will be accepted mostly by the 3s orbital (Figure 6), because the energy of the $3p_z$ orbital is higher. This axial bond is expected to be relatively strong, perhaps comparable in energy terms with the Mg^{2+}–tetrapyrrole electrostatic interaction inferred above. Furthermore, the electron donation from the ligand will cause the central Mg^{2+} ion to be pulled out of the molecular plane due to the increased repulsion between the Mg^{2+} ion and the sp^2 electrons. In hexacoordinated complexes, formed only with strong ligands (Py, Im, MeOH), in order to accommodate another two electrons, the 3s and $3p_z$ orbitals are expected to form two sp hybrids, protruding axially. The complex becomes symmetrical as the CMI is pulled back into the molecular plane. These effects are seen both in crystallographic studies and in the present and previous computations.[48] However, the strength of the axial coordination bonds in the $L-Mg^{2+}-L$ complex will be lowered due to the acceptance of additional electrons by Mg^{2+} at the cost of increased electrostatic repulsion at the core of the complex. This explains the well-known experimental observation that the hexacoordinated state of Mg^{2+} in (B)Chls is thermodynamically less favored.[5] Repulsion at the core seems to be the dominant factor in axial ligand binding to (B)Chls, which is in line with the fact that high pressure pushes the ligation equilibrium toward deligation (see above). Additionally, in hexacoordinated BChla the pressure and repulsion effects seem to compensate for each other, and this explains the insensitivity of the Q_X transition energy to external pressure in this coordination state.

Zn Complexes. Because the 4s, $4p_x$, and $4p_y$ orbitals in Zn^{2+} are engaged in the formation of coordination bonds with the chelator, only the axially oriented $4p_z$ can be the acceptor orbital (Figure 6), and hence pentacoordination will be the favored state of Zn-BPheo complexes. The binding of the second ligand could be achieved only at the expense of the existing bond, as the ligands compete for the same orbital at the metal center. This is consistent with the fact that the coordination state (penta) of the central Zn^{2+} does not change under external pressure. Indeed, coordination of the second axial ligand to the central Zn^{2+} is rarely observed, and the bond is much weaker (longer) as seen, for example, in Zn-porphyrins.[40] As mentioned above, an increase in its length by 0.3–0.4 Å is seen also in our computations.

Ni Complexes. In Ni^{2+} complexes, again only the $4p_z$ orbital is a favored acceptor of an electron pair from the axial ligand (Figure 6), and owing to strong Ni^{2+}–macrocycle bonding, the pentacoordinated complex, with the CMI least shifted from the molecular plane (Table 4), is likely to be the most stable form. Hexacoordination occurs only with strong ligands, such as Py and Im, able to rebuild the electronic structure of the central Ni^{2+} ion, in which the axial and equatorial ligations are mutually correlated.[10] In effect, the d orbitals assume the energetically more favorable electronic configuration $t_{2g}^6e_g^2$, and the ligand field symmetry gains O_h character. Obviously, this requires a rehybridization of the original electronic configuration (see above), and consequently the resulting hexacoordinated high-spin complexes reveal paramagnetism.[8]

Coordination of Water Molecules. The coordination of water molecules to Mg^{2+} chelates is of relevance to many biological systems, and as such, it has been the subject of intensive experimental and theoretical studies.[34] Our results show that a double axial ligation of (B)Chls with water molecules is highly unprivileged, both under high pressure and in media of low permittivity (aqueous ACN). This is in agreement with the results of recent theoretical studies, which predict unfavorable thermodynamic parameters of second ligand binding and point to the part played by dispersion energy and medium polarity in this process.[48,50] The central Mg^{2+}–ligand bond, being mostly of an electrostatic nature, is found to depend on the environment dielectric constant.[32,48,51,52] Intuitively, the tendency to avoid axial coordination of two water molecules can be attributed to several factors. The binding of H_2O to the central Mg^{2+} requires the breakage of H bonds (at an energetic penalty of ~5 kcal/mol[53]) and causes the increase of local order (= a decrease in entropy). When the first H_2O molecule binds, these unfavorable effects are compensated for by a gain in enthalpy of ~7 kcal/mol, due to the formation of a coordination bond. Ligation by single H_2O is then privileged owing to the overall negative ΔG. The energetic effect of a second H_2O molecule binding is lower, in the range 1.5–5 kcal/mol,[5] and it does not compensate for the unfavorable effects. In effect, the hexacoordination of (B)Chls in an aqueous environment is rarely or almost never observed,[46] even under high pressure.

4. CONCLUSIONS

The present analysis shows that the character of bonding between the central metal ion and the macrocyclic tetrapyrrolic chelator depends on both the electronic configuration of the central ion and the symmetry of electron distribution in the

dx.doi.org/10.1021/ic501029b | Inorg. Chem. 2014, 53, 8473–8484

inner cavity. The theoretically predicted types of interactions within the central binding pocket, as based on orbital symmetry analysis, are fully supported experimentally by the solvent and pressure effects on the spectral properties of the metallocomplexes. In general, in complexes with the main group metals (closed-shell configuration), the metal ion−macrocycle interaction is mostly electrostatic, and the resulting complexes are labile. The metal ions with a closed d shell may form classical coordination bonds with the macrocycle, engaging their p and s orbitals. These complexes will be of higher stability. Transition metals, due to the unfilled d shell, do form much more stable complexes, because of strong bonding via both coordination and covalent interactions. Indeed, the XPS measurements show that the electron binding energies at the core nitrogens in metallosubstituted Chls[30] increase progressively as follows: $Mg^{2+} < Zn^{2+} < Ni^{2+}$. These conclusions apply to all metallosubstituted tetrapyrroles, whose molecules do not possess an inversion center (C_1, C_2 and C_{2v} symmetry). In other cases, e.g., in flat metalloporphyrins with D_{4h} symmetry, there will be a strict separation between the central metal ion and the macrocycle.[54] This will not be the case when the central ion shifts out of plane and the complex changes its symmetry to C_{4v}. In the real world, due to, for example, thermally activated molecular distortions and fast dynamic changes in symmetry, as predicted theoretically for Ni-porphyrin,[55] central metal ion−macrocycle bonding will fluctuate, interconverting between different types of bonds, ionic, coordination, and covalent. This bond interconversion is consistent with the DFT-based estimations of core size in metalloporphyrins,[33] which predict the strongest CMI−core nitrogen interaction for Ni^{2+} and somewhat weaker for Zn^{2+}.

Concerning the Mg^{2+} complexes, i.e., (B)Chls, electronic repulsion at the core is a dominant factor in the axial ligand binding. A water molecule is not preferred as their second axial ligand because the weak enthalpic effect of its binding does not compensate for unfavorable entropy change. The consequences of this fact are highly relevant for biological systems where water molecules do not saturate the axial ligand binding sites, which thus facilitates a controlled coordination of amino acid side groups.

5. EXPERIMENTAL SECTION

Pigment Preparation. BPheo was prepared from BChla by short treatment with small amounts of double-distilled glacial acetic acid at room temperature. The acid was evaporated in a stream of nitrogen, and the pigment was purified by column chromatography on DEAE-Sepharose in acetone.[56] Zn-BPheo was prepared by the direct insertion of Zn^{2+} ion into the macrocycle ring, and Ni-BPheo by a transmetalation method, following previously described methods.[8] Zn-BPheo (retention time ∼12 min) was purified by HPLC on a semipreparative silica gel column (Varian, 250 × 4.6 mm) using the following elution program: 0−5 min 3% IPA in *n*-hexane, 5−30 min 2% IPA in *n*-hexane, at a flow rate of 1 mL/min. Ni-BPheo (retention time ∼54 min) was purified by isocratic HPLC on a reversed-phase silica gel column (Varian RP-C18, 250 × 10 mm) using methanol as the eluent at a flow rate of 4 mL/min. Because of the high instability of the pigments, all preparative steps were done as quickly as possible and under dim light.

Reagents. Acetone, acetonitrile, methanol, IPA, and *n*-hexane were of HPLC grade (LabScan, Ireland). Dimethylformamide and pyridine were of spectroscopic grade (Merck, Uvasol, Germany). Imidazole (purity >99.5%) was obtained from Fluka (Germany). All solvents used for the preparation of pigments were of analytical grade (POCh, Gliwice, Poland).

Micellar System. To prepare the solution of pigments in the micellar system, acetone pigment solutions in acetone were added dropwise by vigorous stirring to 2.5 mL of 0.1% Triton X-100 solution in a 20 mM Tris·HCl buffer, until absorbance at the Soret maximum was about 0.5. Then the solutions were titrated with 10% Triton X-10 until equilibria between monomeric and oligomeric forms were established, as judged from the absorption spectra. The final concentration of the detergent was 5.6% and 0.8% in the cases of BPheo and BChla, respectively.

Spectroscopic Measurements. The effects of high hydrostatic pressure on the absorption spectra of BChla were measured on a custom-built high-pressure probe, according to a previously described method.[11] The absorption spectra were measured using a Shimadzu 2101 PC spectrophotometer (Japan) in a range from 350 to 900 nm with a 0.5 nm increment. Each spectrum was recorded in three repetitions, and for the analyses their means were taken. The concentrations of the pigments were about 2×10^{-6} M. The measurements were done at room temperature in a pressure range between 0.1 and 200 MPa.

Analysis of Spectral Data. In order to estimate the contribution from four-, five-, and six-coordinated forms of the pigments, a deconvolution procedure was used, as described previously.[5,11,46] The Q_X regions of the absorption spectra were analyzed using version 4.0 of PeakFit software (Jandel, USA). Prior to fitting, the baseline (flat quadratic function) was subtracted from each spectrum and the second derivative was computed to position the maxima of the absorption bands. As previously, all components were fitted with the same Gaussian−Lorentzian function. The energies of the (0−1) vibrational sidebands of the Q_X transition were placed 1200−1300 cm^{-1} higher than their origins, while their areas were usually 20−25% of the parental transition.

Theoretical Calculations. The computational results were obtained within DFT, as implemented in Turbomole v. 6.3[57] with the gradient-corrected Becke−Perdew (BP) functional.[58−62] This functional proved suitable for a determination of the geometry of magnesium porphyrins, Chls, and BChls.[18,48,53] All electron basis sets of def-TZVP[63] quality were employed for all atoms. The resolution of identity approach was applied to compute the electronic Coulomb interactions.[64,65] A complete geometry optimization was performed for each experimental system (i.e., pigment + ligand(s)). Standard convergence criteria for geometry optimization were applied, i.e., 10^{-6} au for energy, 10^{-3} for the gradient, and 10^{-6} for the root-mean-square of the density matrix. The character of the obtained stationary states was additionally confirmed by frequency calculations. The energies of the electronic excitations of selected BChla complexes were also determined using the TD-DFT method with the BP functional. As a prerequisite, the convergence criteria were tightened to 10^{-6} au for energy and 10^{-8} for density. For each system the 10 lowest singlet excitations were computed. The computations were performed at the Academic Computer Centre Cyfronet AGH on an SGI Altix 3700 supercomputer.

■ ASSOCIATED CONTENT

Ⓢ Supporting Information

A figure (Figure S1) showing the effects of hydrostatic pressure on the absorption spectra of the model complexes and a listing of the shifts of their electronic transitions caused by pressure (Table S1). This material is available free of charge via the Internet at http://pubs.acs.org.

■ AUTHOR INFORMATION

Corresponding Author

*E-mail: leszek.fiedor@uj.edu.pl.

Notes

The authors declare no competing financial interest.

■ ACKNOWLEDGMENTS

The work was in part supported by the Ministry of Science and Higher Education (grant no. N N204 439640 to D.R.Z.), the Polish National Science Centre (grant no. DEC-2012/05/B/ST5/00389 to G.S.), and by the Foundation for Polish Science (grant no. TEAM/2010-5/3 to L.F.). The computational time at the Academic Computer Centre Cyfronet AGH is acknowledged (grant no. MNiSW/IBM_BC_HS21/PAN/033/2012). D.R.Z. received funding from the Marian Smoluchowski Krakow Research Consortium, a Leading National Research Centre KNOW supported by the Ministry of Science and Higher Education. The Faculty of Biochemistry, Biophysics and Biotechnology of the Jagiellonian University is a beneficiary of structural funds from the European Union (grant no. POIG.02.01.00-12-064/08, "Molecular Biotechnology for Health"). The authors are grateful to Prof. Rudi van Eldik for fruitful discussions and to Mr. Zygmunt Wołek for his assistance with the high-pressure measurements.

■ REFERENCES

(1) Küpper, H.; Dedic, R.; Svoboda, A.; Hala, J.; Kroneck, P. M. H. *Biochim. Biophys. Acta* **2002**, *1572*, 107−113.
(2) Drzewiecka-Matuszek, A.; Skalna, A.; Karocki, A.; Stochel, G.; Fiedor, L. *J. Biol. Inorg. Chem.* **2005**, *10*, 453−462.
(3) Küpper, H.; Küpper, F. C.; Spiller, M. [Heavy metal]-Chlorophylls formed in vivo during metal stress and degradation products formed during digestion, extraction and storage of plant material. In *Chlorophylls and Bacteriochlorophylls*; Grimm, B.; Porra, R. J.; Rüdiger, W.; Scheer, H., Eds.; Springer: Dordrecht, 2006; Vol. *25*, pp 67−77.
(4) Noy, D.; Yerushalmi, R.; Brumfeld, V.; Ashur, I.; Scheer, H.; Baldridge, K. K.; Scherz, A. *J. Am. Chem. Soc.* **2000**, *122*, 3937−3944.
(5) Kania, A.; Fiedor, L. *J. Am. Chem. Soc.* **2006**, *128*, 454−458.
(6) Evans, T. A.; Katz, J. J. *Biochim. Biophys. Acta, Bioenerg.* **1975**, *396*, 414−426.
(7) Callahan, P. M.; Cotton, T. M. *J. Am. Chem. Soc.* **1987**, *109*, 7001−7007.
(8) Hartwich, G.; Fiedor, L.; Simonin, I.; Cmiel, E.; Schäfer, W.; Noy, D.; Scherz, A.; Scheer, H. *J. Am. Chem. Soc.* **1998**, *120*, 3675−3683.
(9) Ashur, I.; Brandis, A.; Greenwald, M.; Vakrat-Haglili, Y.; Rosenbach-Belkin, V.; Scheer, H.; Scherz, A. *J. Am. Chem. Soc.* **2003**, *125*, 8852−8861.
(10) Yerushalmi, R.; Noy, D.; Baldridge, K. K.; Scherz, A. *J. Am. Chem. Soc.* **2002**, *124*, 8406−8415.
(11) Fiedor, L.; Kania, A.; Mysliwa-Kurdziel, B.; Stochel, G. *Biochim. Biophys. Acta* **2008**, *1777*, 1491−1500.
(12) Orzeł, Ł.; Fiedor, L.; Wolak, M.; Kania, A.; van Eldik, R.; Stochel, G. *Chem.—Eur. J.* **2008**, *14*, 9419−9430.
(13) Fiedor, J.; Pilch, M.; Fiedor, L. *J. Phys. Chem. B* **2009**, *113*, 12831−12838.
(14) Orzeł, Ł.; Kania, A.; Rutkowska-Zbik, D.; Susz, A.; Stochel, G.; Fiedor, L. *Inorg. Chem.* **2010**, *49*, 7362−7371.
(15) Pilch, M.; Dudkowiak, A.; Jurzyk, B.; Łukasiewicz, J.; Susz, A.; Stochel, G.; Fiedor, L. *Biochim. Biophys. Acta* **2013**, *1827*, 30−37.
(16) Noy, D.; Fiedor, L.; Hartwich, G.; Scheer, H.; Scherz, A. *J. Am. Chem. Soc.* **1998**, *120*, 3684−3693.
(17) Sundholm, D. *Chem. Phys. Lett.* **1999**, *302*, 480−484.
(18) Heimdal, J.; Jensen, K.; Devarajan, A.; Ryde, U. *J. Biol. Inorg. Chem.* **2007**, *12*, 49−61.
(19) Petke, J. D.; Maggiora, G. M.; Shipman, L. L.; Christoffersen, R. E. *Photochem. Photobiol.* **1979**, *30*, 203−223.
(20) Petke, J. D.; Maggiora, G. M.; Shipman, L. L.; Christoffersen, R. E. *Photochem. Photobiol.* **1980**, *32*, 399−414.
(21) Hanson, L. K. Molecular orbital theory of monomer pigments. In *Chlorophylls*; Scheer, H., Ed.; CRC Press: Boca Raton, 1991; pp 993−1012.
(22) Sundholm, D. *Chem. Phys. Lett.* **2000**, *317*, 545−552.
(23) Linnanto, J.; Korppi-Tommola, J. *J. Comput. Chem.* **2004**, *25*, 123−137.
(24) Linnanto, J.; Korppi-Tommola, J. *Phys. Chem. Chem. Phys.* **2006**, *8*, 663−687.
(25) Zucchelli, G.; Brogioli, D.; Casazza, A. P.; Garlaschi, F. M.; Jennings, R. C. *Biophys. J.* **2007**, *93*, 2240−2254.
(26) Smith, K. M. *Porphyrins and Metalloporphyrins*; Elsevier: Amsterdam, 1975.
(27) Dolphin, D. *The Porphyrins*; Academic Press: New York, 1978.
(28) Enikolopyan, N. S. *Porphyrins: Spectroscopy, Electrochemistry and Applications (in Russian)*; Nauka, 1987.
(29) Kadish, K. M.; Smith, K. M.; Guilard, R. *The Porphyrin Handbook*; Academic Press: Amsterdam, 2000.
(30) Nonomura, Y.; Igarashi, S.; Yoshioka, N.; Inoue, H. *Chem. Phys.* **1997**, *220*, 155−166.
(31) Liao, M.-S.; Scheiner, S. *J. Chem. Phys.* **2002**, *117*, 205−219.
(32) Petit, L.; Adamo, C.; Russo, N. *J. Phys. Chem. B* **2005**, *109*, 12214−12221.
(33) Kozlowski, P. M.; Bingham, R. J.; Jarzecki, A. A. *J. Phys. Chem. A* **2008**, *112*, 12781−12788.
(34) Barkigia, K. M.; Fajer, J. Models of photosynthetic chromophores: molecular structures of chlorins and bacteriochlorins. In *The Photosynthetic Reaction Center*; Deisenhofer, J.; Norris, J. R., Eds.; Academic Press, Inc.: San Diego, 1993; Vol. *2*, pp 513−539.
(35) Deisenhofer, J.; Michel, H. *Annu. Rev. Biophys. Biophys. Chem.* **1991**, *20*, 247−266.
(36) McDermott, G.; Prince, S. M.; Freer, A. A.; Hawthornthwaite-Lawless, A. M.; Papiz, M. Z.; Cogdell, R. J.; Isaacs, N. W. *Nature* **1995**, *374*, 517−521.
(37) Liu, Z.; Yan, H.; Wang, K.; Kuang, T.; Zhang, J.; Gui, L.; An, X.; Chang, W. *Nature* **2004**, *428*, 287−292.
(38) Jordan, P.; Fromme, P.; Witt, H. T.; Klukas, O.; Saenger, W.; Krauss, N. *Nature* **2001**, *411*, 909−917.
(39) Ferreira, K. N.; Iverson, T. M.; Maghlaoui, K.; Barber, J.; Iwata, S. *Science* **2004**, *303*, 1831−1838.
(40) Schauer, C. K.; Anderson, O. P.; Eaton, S. S.; Eaton, G. R. *Inorg. Chem.* **1985**, *24*, 4082−4086.
(41) Barkigia, K. M.; Miura, M.; Thompson, M. A.; Fajer, J. *Inorg. Chem.* **1991**, *30*, 2233−2236.
(42) Song, Y.; Haddad, R. E.; Jia, S.-L.; Hok, S.; Olmstead, M. M.; Nurco, D. J.; Schore, N. E.; Zhang, J.; Ma, J.-G.; Smith, K. M.; Gazeau, S.; Pecaut, J.; Marchon, J.-C.; Medforth, C. J.; Shelnutt, J. A. *J. Am. Chem. Soc.* **2005**, *127*, 1179−1192.
(43) Ellervee, A.; Freiberg, A. *Chem. Phys. Lett.* **2008**, *450*, 386−390.
(44) Ellervee, A.; Linnanto, J.; Freiberg, A. *Chem. Phys. Lett.* **2004**, *394*, 80−84.
(45) Bruins, M. E.; Janssen, A. E. M.; Boom, R. M. *J. Mol. Catal. B: Enzym.* **2006**, *39*, 124−127.
(46) Fiedor, L. *Biochemistry* **2006**, *45*, 1910−1918.
(47) Singh, A.; Johnson, L. W. *Spectrochim. Acta, Part A* **2002**, *58*, 1573−1576.
(48) Rutkowska-Zbik, D.; Korona, T. *J. Chem. Theory Comput.* **2012**, *8*, 2972−2982.
(49) Rutkowska-Zbik, D.; Witko, M. *J. Mol. Model.* **2013**, *19*, 4155−4161.
(50) Ben Fredj, A.; Ben Lakhdar, Z.; Ruiz-López, M. F. *Chem. Phys. Lett.* **2009**, *472*, 243−247.
(51) Dudev, T.; Lim, C. *Chem. Rev.* **2003**, *103*, 773−787.
(52) Petit, L.; Quartarolo, A.; Adamo, C.; Russo, N. *J. Phys. Chem. B* **2006**, *110*, 2398−2404.
(53) Rutkowska-Zbik, D.; Witko, M.; Fiedor, L. *J. Mol. Model.* **2013**, *19*, 4661−4667.
(54) Zamyatin, A. V.; Gusev, A. V.; Rodgers, M. A. J. *J. Am. Chem. Soc.* **2004**, *126*, 15934−15935.
(55) Rush, T. S.; Kozlowski, P. M.; Piffat, C. A.; Kumble, R.; Zgierski, M. Z.; Spiro, T. G. *J. Phys. Chem. B* **2000**, *104*, 5020−5034.
(56) Fiedor, L.; Rosenbach-Belkin, V.; Scherz, A. *J. Biol. Chem.* **1992**, *267*, 22043−7.

(57) *TURBOMOLE* V6.3 2011, a. d. o. U. o. K. a.; Forschungszentrum Karlsruhe GmbH; TURBOMOLE GmbH, s. a. f.; http://www.turbomole.com.
(58) Dirac, P. A. M. *Proc. R. Soc. London, Ser. A* **1929**, *123*, 714−733.
(59) Slater, J. C. *Phys. Rev.* **1951**, *81*, 385−390.
(60) Vosko, S. H.; Wilk, L.; Nusair, M. *Can. J. Phys.* **1980**, *58*, 1200−1211.
(61) Becke, A. D. *Phys. Rev. A* **1988**, *38*, 3098−3100.
(62) Perdew, J. P. *Phys. Rev. B* **1986**, *33*, 8822−8824.
(63) Schäfer, A.; Huber, C.; Ahlrichs, R. *J. Chem. Phys.* **1994**, *100*, 5829−5835.
(64) Eichkorn, K.; Treutler, O.; Öhm, H.; Häser, M.; Ahlrichs, R. *Chem. Phys. Lett.* **1995**, *240*, 283−289.
(65) Eichkorn, K.; Weigend, F.; Treutler, O.; Ahlrichs, R. *Theor. Chem. Acc.* **1997**, *97*, 119−124.

■ NOTE ADDED AFTER ASAP PUBLICATION

This paper was published on the Web on July 29, 2014, with the fifth author name being incorrect. The corrected version was reposted on July 30, 2014.